

Synthesis of mesoporous SBA-15/ionic liquid nanocomposites for the selective oxidation of 2,3,6-trimethylphenol

Nurliana Roslan^a, Hendrik O. Lintang^{b,c}, Salasiah Endud^a, Mohd Bakri Bakar^a and Zainab Ramli^{a*}

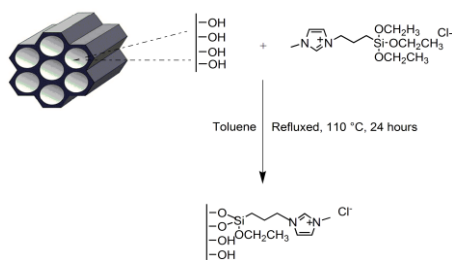
^aDepartment of Chemistry, Faculty of Science, Universiti Teknologi Malaysia, 81310 Johor Bahru, Johor, Malaysia, ^bCentre of Sustainable Nanomaterials, Ibnu Sina Institute for Scientific and Industrial Research, Universiti Teknologi Malaysia, 81310 Johor Bahru, Johor, Malaysia, ^cMa Chung Research Center for Photosynthetic Pigments, Universitas Ma Chung, 65151 Malang, Indonesia, *Corresponding Author: zainab@kimia.fs.utm.my

Article history :

Received 22 September 2016

Accepted 30 October 2016

GRAPHICAL ABSTRACT



ABSTRACT

We report the grafting of ILs onto mesoporous silica SBA-15 nanomaterial with a larger surface area of 737.96 m²/g and an interpore distance of 10.68 nm for selective oxidation of 2,3,6-trimethylphenol (TMP). IL, 1-(3-(triethoxysilyl)propyl)-3-methylimidazolium chloride was grafted with concentration of 1.0, 2.0, 4.0, 6.0, 8.0 and 10.0 mmol onto SBA-15 via a sol-gel method to obtain IL-SBA-15 nanocomposites. The appearance of vibration bands of C-H (~2900 cm⁻¹), C=C (~1630 cm⁻¹) and C=N bonds (~1570 cm⁻¹) in the FTIR spectra indicates that the ILs were successfully grafted on the surface of SBA-15. The total surface area, total pore volume and BJH pore size distribution of all IL-SBA-15 nanocomposites decreasing with the increasing amount of IL from 393.27 to 354.39 m²/g which indicated that the pore channel and/or surface of SBA-15 were occupied by IL without significant reduction of the quality. It was found that the grafted amount of IL on SBA-15 nanocomposites increased from 0.60 to 0.97 mmol/g when amount of ILs content in the mixture was increased from 1.0 to 10.0 mmol. The IL-SBA-15 nanocomposites were tested as a heterogeneous catalyst for oxidation reaction of 2,3,6-TMP to 2,3,5-trimethylbenzoquinone (TMBQ), employing *tert*-butyl hydroperoxide (TBHP) as an oxidant at 80 °C for 24 hours. All IL-SBA-15 nanocomposites gave 100% selectivity towards 2,3,5-TMBQ in which IL-SBA-15 with 1.0 mmol of IL gave the highest conversion of TMP (37%).

Keywords: Ionic liquid, SBA-15, Nanocomposites, Oxidation, 2,3,6-Trimethylphenol

© 2016 Dept. of Chemistry, UTM. All rights reserved
| eISSN 0128-2581 |

1. INTRODUCTION

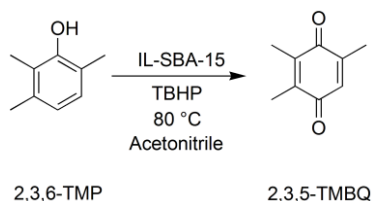
Ionic liquids (ILs) are organic salts which combine good tunable solubility properties with low melting points, a negligible vapour pressure, high ionic conductivity, non-flammability, wide liquid range up to 300 °C and ability to dissolve a variety of organic and inorganic compounds [1,2]. Moreover, in some cases ILs also showed similar problems to homogeneous catalyst such as miscible with some products or reactant, leaving separation and reuse of catalyst [3]. Thus, ILs functionalized porous materials have been shown as an alternative way that drawn considerable attention for the development of heterogeneous catalysts. Porous materials are most commonly used as an attractive inorganic support due to their outstanding texture parameters such as various pore morphologies, pore structure, framework composition, high specific surface area and large pore volume [4].

Mesoporous SBA-15 materials are one of porous structures that have attracted great interest due to their large surface area, large pore volume, high ordered channel structures with uniform pore diameter (3-30 nm), high hydrothermal stability and possesses thicker wall [5,6]. These features make mesoporous SBA-15 as suitable

supports for grafting of ILs because the presence of mesopores would facilitate accessibility of bulky reactant molecules to the catalytic sites [7].

Selective oxidation of phenols to quinones is one of the attractive transformations in organic chemistry because it has been widely used as intermediates in the synthesis of fine chemicals and pharmaceuticals [8]. 2,3,5-trimethylbenzoquinone (TMBQ) represents an important intermediate for the industrial production of vitamin E (α -tocopherol), which is used extensively as antioxidant in food, medical treatments and cosmetics [9]. The current or traditional procedure of the 2,3,5-TMBQ production in industry involves *para*-sulfonation of 2,3,6-TMP, followed by oxidation with MnO₂ and reduction from 2,3,6-TMP. This procedure, however, has considerable limitations including high cost and generates a large amount of solid and liquid wastes due to the use of sulfuric acid and stoichiometric solid oxidants as well as reductants [10]. So far, copper halides and other copper salts, cobalt complexes with Schiff bases, ruthenium salts and heteropoly acids have been extensively reported as catalysts for the oxidation of 2,3,6-TMP. Therefore, in this research work, a series of heterogeneous catalyst of IL-SBA-15 nanocomposites for the one-step oxidation of 2,3,6-TMP to 2,3,5-TMBQ was

used as model reaction in the presence of TBHP as oxygen source as shown in Scheme 1.



Scheme 1 Catalytic oxidation of 2,3,6-TMP to 2,3,5-TMBQ over IL-SBA-15 nanocomposites

2. EXPERIMENTAL

2.1 Preparation of Ionic Liquid (IL)

1-(3-triethoxysilylpropyl)-3-methylimidazolium chloride (IL) was prepared according to the procedure reported elsewhere [11] with some modification by heating N-methylimidazole (25 mmol) and (3-chloropropyl) triethoxysilane (25 mmol) at 110 °C for 40 hours. Then, the unreacted materials were washed by diethyl ether (8 mL x 3) and removed under reduced pressure at room temperature. Finally, yellowish viscous ionic liquid was obtained (21.08 mmol; 6.5533g).

2.2 Preparation of Mesoporous Silica SBA-15

Mesoporous silica SBA-15 was synthesized according to the procedure reported by Zhao *et al.* [12]. Typically, 4.00 g of Pluronic P123, EO₂₀PO₇₀EO₂₀ (0.69 mmol) was dissolved in 30 g of distilled water and 120 g of 2 M hydrochloric acid (HCl) with stirring at 35 °C. Tetraethyl orthosilicate, 8.50 g of TEOS (22.8 mmol) was then added into the solution with stirring at 35 °C. After 20 hours, the mixture was aged in the oven at 100 °C for 24 hours without stirring. The white solid product was filtered and washed with distilled water, followed by the drying at room temperature. The as-synthesized SBA-15 was then extracted by Soxhlet extractor in the mixture of distilled water and ethanol (95 %) for 18 hours and the final powder of SBA-15 was obtained (2.692 g).

2.3 Preparation of IL-SBA-15 Nanocomposites

For the preparation of IL grafted SBA-15 (xIL-SBA-15 with x as mmol of IL), IL with x in 1.0, 2.0, 4.0, 6.0, 8.0, 10.0 mmol was added dropwise into the suspension of SBA-15 (1.00 g) in dried toluene (50 mL). The resulting mixtures were then refluxed at 110 °C for 24 hours under nitrogen condition. After cooling to room temperature, the resulting solid was recovered and washed with anhydrous ethanol. The adsorptive ionic liquid was removed by Soxhlet extraction technique for 48 hours and then dried at room temperature under vacuum condition [13].

2.4 Characterizations

SBA-15 and IL-SBA-15 nanocomposites were characterized by Fourier-transform infrared spectra (FT-IR) spectroscopy on Perkin Elmer Spectrum One FT-IR with KBr pellet technique. Spectra were recorded between 4000 and 450 cm⁻¹ at a resolution of 4 cm⁻¹. The pore size distribution, pore volume and specific surface area of the materials were determined from a N₂ adsorption-desorption isotherms analysis at 77 K using a Micromeritics ASAP 2010. The thermal gravimetric analysis was performed by using Perkin Elmer Pyris Diamond TG/DTA 6300 Thermal Analyzer under nitrogen flow.

2.5 Catalytic Activity

2,3,6-TMP was used as the model reactant for the epoxidation reaction by TBHP as oxidant. A typical reaction mixture was carried out in a round bottom flask as follows: a 50 mg catalyst, 5 mmol of TBHP (70%), 1.25 mmol of TMP and ethyl benzoate (0.25 mmol) as an internal standard was mixed in a 10 mL of acetonitrile as solvent. Then the reaction mixture was heated at 80 °C and stirred for 24 hours. A blank reaction was carried out as control, by using SBA-15 and IL as catalyst. The products of the reaction were analyzed by Agilent Gas chromatography model 7890N equipped with flame ion detector (FID) using an Ultra 1 column and a GC-MS instrument.

3. RESULTS AND DISCUSSION

3.1 Characterizations of materials

Figure 1 shows the FT-IR spectra of pure SBA-15 and IL-SBA-15 nanocomposites with various amount of IL loading. As shown in the SBA-15 spectrum, the vibration bands observed at 1085 and 804 cm⁻¹ were assigned to the asymmetric Si-O-Si, ν_{as}(Si-O-Si) and symmetric stretching Si-O-Si, ν_s(Si-O-Si) vibrations of the silica framework, respectively. Moreover, vibration band at 1638 cm⁻¹ revealed as bending vibration of water O-H bonds in OH groups, while symmetric stretching vibration of free silanol (Si-OH) groups on the surface of the silica was assigned at 958 cm⁻¹. The bending vibration mode of Si-O-Si, δ(Si-O-Si) was observed at 465 cm⁻¹. On the other hand, the IL-SBA-15 spectra with different concentration of IL also showed similar characteristics and trend of the SBA-15 framework. It can be seen that the vibration bands at 1639 and 1575 cm⁻¹ were assigned to the characteristic absorbance for skeleton vibrations of the imidazolium ring (C=N and C=C bonds). Meanwhile, the modification of the SBA-15 by IL was reflected in the FT-IR spectra by the presence of asymmetric and symmetric -CH₂ stretching bands at the 2958 and 2929 cm⁻¹. Another important feature is that the vibration band at 1460 cm⁻¹ is due to the deformation vibration of imidazole part and alkyl chain. From the IL-SBA-15 spectra, the intensity of the vibration band around

950 cm^{-1} , which is attributed to the symmetric Si-OH stretching, was slightly decreased due to the modification of IL. Thus, these results confirm that ILs were successfully grafted on the surface of silanol group of SBA-15.

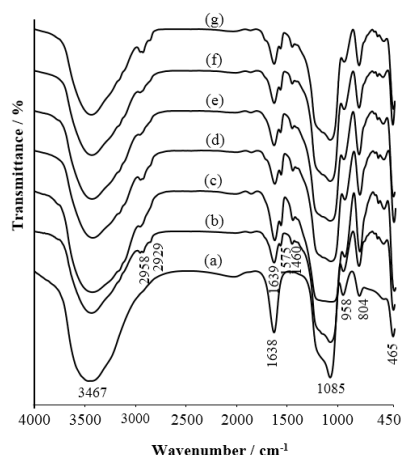


Figure 1 FTIR spectra of (a) SBA-15, (b) 1.0 IL-SBA-15, (c) 2.0 IL-SBA-15, (d) 4.0 IL-SBA-15, (e) 6.0 IL-SBA-15 (f) 8.0 IL-SBA-15 and (g) 10.0 IL-SBA-15

Thermogravimetric analysis (TGA) for the IL-SBA-15 nanocomposites samples was performed in the temperature range of 40 to 800 °C. Based on the TGA thermograms presented in Figure 2, there are 4 different stages of thermal events. It can be seen that there is an initial loss of weight at temperature below 100 °C for all samples which was due to the removal of physically adsorbed water or any minor solvent residues remaining from the particle modification process. However, physically adsorbed water was removed completely when the samples undergo further heating to about 100 °C. On the other hand, IL-SBA-15 showed weight loss occurred between 100 – 250 °C and 250 – 400 °C, were attributed to the decomposition of organic moieties (IL) in SBA-15 [14,15]. Beyond this temperature, in the range 400 – 800 °C, the residual ethoxy side groups are decomposed [16, 17]. As shown in Table 1, the total weight losses for IL-SBA-15 at temperature range from 40 to 800 °C were increased from 22.7% to 29.3%, respectively. All TGA thermograms clearly indicate that IL is well anchored over the modified surface of SBA-15. Moreover, the higher mass loss observed for the 10.0 IL-SBA-15 (Figure 2f) nanocomposite shows the larger amount of IL (organic parts) anchored on the surface of SBA-15. In this case of 10.0 IL-SBA-15 sample (Figure 2f), a highest total weight loss of 13.1% was noticed, which was due to the complete decomposition of the IL moieties heterogenized over SBA-15. On the other hand, TGA was also employed to calculate the grafted amount of IL based on the weight loss between 100 °C and 800 °C, $W_{100-800}$, where M (g/mol) is the molecular weight of the grafted IL moieties (Equation 1) [18]. From Table 1, the grafted amount of IL increased obviously from 0.60 to 0.97 mmol/g with the increase of the IL concentration in the initial mixture from 1 to 10 mmol. In order to calculate the grafted yield which is corresponding

to the percentage of IL molecules that successfully grafted on the SBA-15, the following equation 2 is employed as shown below [19]. It was also found that the grafted yield decreases continuously from 60.0 to 9.7% as the concentration of IL increases. These results confirmed that the IL moieties is chemically grafted on the SBA-15 and not physically absorbed.

$$\text{Grafted amount (mmol/g)} = \frac{10^3 W_{100-800}}{M(100 - W_{100-800})} \quad (1)$$

$$\text{Grafted yield (\%)} = \frac{\text{Grafted amount}}{\text{IL concentration}} \times 100\% \quad (2)$$

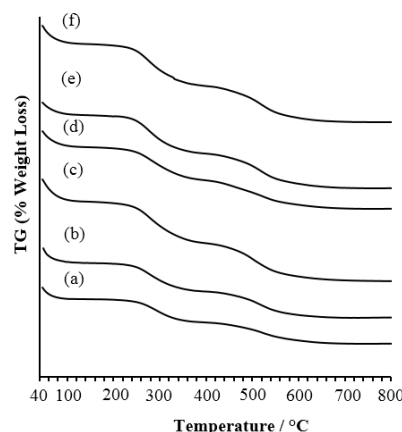


Fig. 2 TGA thermograms of (a) 1.0 IL-SBA-15, (b) 2.0 IL-SBA-15, (c) 4.0 IL-SBA-15, (d) 6.0 IL-SBA-15, (e) 8.0 IL-SBA-15 and (f) 10.0 IL-SBA-15.

Table 1 TGA data of IL-SBA-15 nanocomposites

Samples	Weight loss (%) ^a	The grafted amount of IL (mmol/g) ^b	Grafted yields (%) ^c
1.0 IL-SBA-15	16.3	0.60	60.0
2.0 IL-SBA-15	17.4	0.65	32.5
4.0 IL-SBA-15	19.0	0.73	18.3
6.0 IL-SBA-15	16.3	0.60	10.0
8.0 IL-SBA-15	23.1	0.93	11.6
10.0 IL-SBA-15	23.9	0.97	9.7

^atotal weight loss between 100 °C and 800 °C. ^bThe grafted amount was calculated by Equation 1 based on TGA. ^cThe grafted yield was calculated by Equation 2 based on TGA.

The textural characteristics of the IL-SBA-15 nanocomposites using different concentration of IL were further identified by N_2 adsorption-desorption analysis as shown in Figure 3. BET specific surface area and Barret-Joyner-Halenda (BJH) distribution were calculated using nitrogen adsorption at 77 K. Figure 3 clearly shows that the characterization of the samples via N_2 adsorption-desorption isotherms possess a similar trend after the surface functionalization. The SBA-15 displayed a typical type IV isotherm with a clear adsorption-desorption H1 hysteresis loop in IUPAC classification and a narrow step occurs approximately at partial pressure $P/P_0 = 0.50-0.75$, characteristics of highly ordered mesoporous materials with

uniform cylindrical pores [20]. For IL-SBA-15 nanocomposites, all samples also exhibited a type IV isotherm with a H1 hysteresis loop with a lower BET specific surface area and a slightly smaller pore volume in comparison with SBA-15. This suggests that the mesoporous structure of SBA-15 was successfully retained during the functionalization. As the concentration of the IL content increases from 1.0 to 10.0 mmol, the surface area decreases considerably compared to SBA-15, which is consistent with the increasing distribution of IL moieties in the interior mesopore surfaces [21]. The BET specific surface area, S_{BET} of IL-SBA-15 was decreased remarkably from 393.93 to 365.00 m^2g^{-1} , respectively, with increases of IL content up to 10 mmol may be due to the bulk chemical structure of IL. On the other hand, shown in Figure 4 are the BJH pore size distribution curves of SBA-15 and IL-SBA-15 nanocomposites which were calculated using the Barrett-Joyner-Halenda model. It can be seen that all IL-SBA-15 samples exhibit a uniform pore size distribution at 3-5 nm. Moreover, IL-SBA-15 samples possess a lower pore size compared than the SBA-15 with a slightly broader distribution and a lower intensity thus indicated a less ordered pore structure. Therefore, these reductions were consistent with the previous works and indicating the presence of IL which was successfully grafted into the SBA-15 [22].

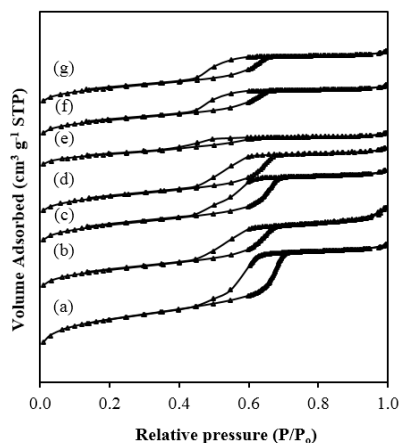


Fig. 3 Nitrogen adsorption-desorption isotherms of (a) SBA-15, (b) 1.0 IL-SBA-15, (c) 2.0 IL-SBA-15, (d) 4.0 IL-SBA-15, (e) 6.0 IL-SBA-15 (f) 8.0 IL-SBA-15 and (g) 10.0 IL-SBA-15.

Table 2 Textural parameters of SBA-15 and IL-SBA-15 nanocomposites

Samples	S_{BET}^a (m^2g^{-1})	S_{Meso}^b (m^2g^{-1})	V_{Total}^c (cm^3g^{-1})	$D_{BJH,Des}^d$ (nm)
SBA-15	737.96	520.25	0.67	5.26
1.0 IL-SBA-15	393.93	304.93	0.48	4.27
2.0 IL-SBA-15	379.65	291.04	0.44	4.82
4.0 IL-SBA-15	363.04	283.28	0.40	4.26
6.0 IL-SBA-15	310.96	214.72	0.24	3.79
8.0 IL-SBA-15	354.39	247.88	0.33	3.77
10.0IL-SBA-15	365.00	260.50	0.34	3.80

^atotal surface area calculated by using the Brunauer-Emmett-Teller (BET) model; ^bmesopore surface area; ^ctotal pore volume based on the desorption total pore volume; ^dpore diameter calculated from the desorption isotherm by using the BJH model.

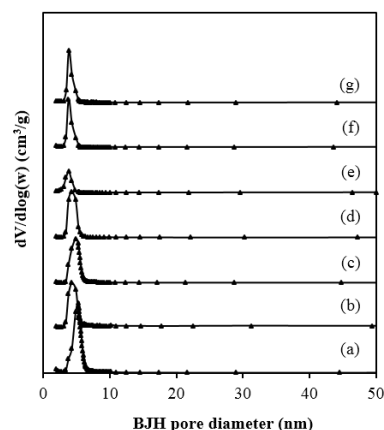


Fig. 4 BJH pore size distribution of (a) SBA-15, (b) 1.0 IL-SBA-15, (c) 2.0 IL-SBA-15, (d) 4.0 IL-SBA-15, (e) 6.0 IL-SBA-15 (f) 8.0 IL-SBA-15 and (g) 10.0 IL-SBA-15.

3.2 Catalytic Studies

The performances of IL-SBA-15 nanocomposites in the one-step oxidation of 2,3,6-TMP when TBHP was used as oxidant and acetonitrile as solvent at 80 °C for 24 hours are shown in Figure 5. A blank experiment was performed in identical conditions, but in absence of catalyst. In this case, the oxidation reaction occurs at very low rate which obtaining a final conversion of 2.1% after 24 hours. The catalytic reactions over SBA-15 and IL have also been carried out for the comparison. As it can be seen, the SBA-15 was not catalytically active in the oxidation of 2,3,6-TMP with 4.8% conversion. For the IL (homogeneous system), it gave higher conversion about 49.6% than the SBA-15. After the functionalization with SBA-15, the conversion of IL-SBA-15 nanocomposites was decreased to 37%. Since IL-SBA-15 nanocomposites are heterogeneous catalyst which means in other words, it can be recycled and reused after the reaction, such decreasing in around 12% is not significantly effect on the performance. In addition, IL and all IL-SBA-15 nanocomposites gave 100% selectivity towards expected product which is 2,3,5-TMBQ. According to the results presented in Figure 5, it is obvious that the percentage conversion of 2,3,6-TMP using IL-SBA-15 nanocomposites were decreased continuously from 1.0 IL-SBA-15 (37.3%) to 10.0 IL-SBA-15 (24.9%) with the increasing of concentration of IL. On the other hand, 1.0 IL-SBA-15 seems to be considerably more active than the other nanocomposites due to the lowest concentration of IL. The pore of IL-SBA-15 maybe clogged as the IL content increase and the reactant (2,3,6-TMP) cannot enter the pore. Thus, the surface area of the IL-SBA-15 nanocomposites plays an important role which provides higher opportunity for the reactant to be catalyzed. Moreover, the 1.0 IL-SBA-15 gave such high yield due to high grafted yield (60%) of IL on the surface of SBA-15. 1.0 IL-SBA-15 nanocomposite might be used not only as heterogeneous catalyst in oxidation reaction but also as support for metalloporphyrins (work in this direction is in progress).

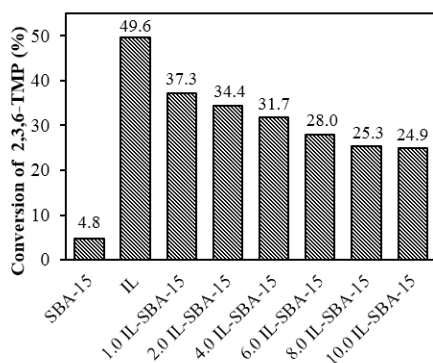


Fig. 5 Conversion of IL-SBA-15 nanocomposites towards oxidation of 2,3,6-TMP

4. CONCLUSION

In summary, IL-SBA-15 nanocomposites were successfully synthesized through sol-gel procedure and characterized by FT-IR, TGA and N₂ adsorption-desorption analysis. The FT-IR analysis indicated that the framework of SBA-15 still preserved after the functionalization with IL. The surface area, total pore volume and average pore size distribution of IL-SBA-15 nanocomposites decreased considerably compared to SBA-15, which is consistent with presence of the functionalized IL. TGA curves of IL-SBA-15 indicated that the weight loss and the grafted amount of IL loading on the surface of SBA-15 were increased with the increase of IL content. All IL-SBA-15 nanocomposites were tested in the oxidation of 2,3,6-TMP using TBHP as oxidant. In the catalytic reaction, all IL-SBA-15 nanocomposites showed as active heterogeneous catalyst in the oxidation of 2,3,6-TMP with only decreasing in small performance compared to the homogeneous one and it gave 100 % selectivity towards 2,3,5-TMBQ.

ACKNOWLEDGEMENT

The authors gratefully acknowledge the Ministry of Education Malaysia for the financial support through GUP Research Grant no. Q.J130000.2526.11H47, myPhd scholarship under MyBrain15 Scheme for Nurliana Roslan, Centre for Sustainable Nanomaterials (CSNano), Ibnu Sina Institute for Scientific and Industrial Research (ISI-SIR), University Industry Research Laboratory (UIRL) and Faculty of Science, Universiti Teknologi Malaysia for research facilities.

REFERENCES

- [1] C.V. Doorslaer, J. Wahlen, P. Mertens, K. Binnemans, D.D. Vos, Dalton Trans. 39 (2010) 8377.
- [2] R. Kurane, J. Jadhav, S. Khanapure, R. Salunkhe, G. Rashinkar, Green Chem 15 (2013) 1849.
- [3] L-W. Xu, M-S. Yang, J-X. Jiang, H-Y. Qiu, G-Q. Lai, Cent. Eur. J. Chem 4 (2007) 1073-1083.
- [4] X. Zhou, A. Duan, Z. Zhao, Y. Gong, H. Wu, Y. Wei, G. Jiang, J. Liu, Mater. Lett. 133 (2014) 228.
- [5] A.S. Cattaneo, C. Ferrara, D.C. Villa, S. Angioni, C. Milanese, D. Capsoni, S. Grandi, P. Mustarelli, V. Allodi, G. Mariotto, S. Brutti, E. Quartarone, Micropor. Mesopor. Mat. 291 (2016) 219.
- [6] G.M. Ziarani, N. Lashgari, A. Badiei, J. Mol. Catal. A: Chem. 397 (2015) 166.
- [7] J. Zhang, G-F. Zhao, Z. Popovic, Y. Lu, Y. Liu, Mater. Res. Bull. 45 (2010) 1648.
- [8] C. Saux, L.R. Pizzio, L.B. Pierella, Appl. Catal. A: Gen. 452 (2013) 17.
- [9] K. Moller, G. Wienhofer, F. Westerhaus, K. Junge, M. Beller, Catal. Today 173 (2011) 68.
- [10] H. Sun, X. Li, J. Sundermeyer, J. Mol. Catal. A: Chem. 240 (2005) 119.
- [11] S. Kumar, S.L. Jain, New J. Chem. 37 (2013) 3057.
- [12] D. Zhou, Q. Huo, J. Feng, B.F. Chmelka, G.D. Stucky, J. Am. Chem. Soc. 120 (1988) 6024.
- [13] X. Sheng, Z. Yuming, Y. Yang, Y. Zhang, Z. Zhang, S. Zhou, X.Fu, S. Zhao, RSC Adv. 4 (2014) 30697.
- [14] X. Wan, M. Tian, K.H. Row, J. Anal. Chem. 65 (2010) 798.
- [15] Q. Wang, G.A. Baker, S.N. Baker, L.A. Colón, The Analyst 131 (2006) 1000.
- [16] A.R. Kiasat, M.J. Nasab, RSC Adv.5 (2015) 75491.
- [17] P. Sharma, A.P. Singh, RSC Adv. 4 (2014) 58467.
- [18] W. He, D. Wu, J. Li, K. Zhang, Y. Xiang, L. Long, S. Qin, J. Yu, Q. Zhang, Bull. Korean Chem. Soc. 34 (2013) 2747.
- [19] W. He, Y. Yao, M. He, Z. Kai, L. Long, M. Zhang, S. Qin, J. Yu, Bull. Korean Chem. Soc. 34 (2013) 112.
- [20] Sing, Physical and Biophysical Chemistry Division Commission on Colloid and Surface Chemistry Including Catalysis, Pure Appl. Chem. 57 (1985) 603.
- [21] Y. Liu, J. Peng, S. Zhai, J. Li, J. Mao, M. Li, H. Qiu, G. Lai, Eur. J. Inorg. Chem. (2006) 2947.
- [22] W. Ding, W. Zhu, J. Xiong, L. Yong, A. Wei, M. Zhang, H. Li, Chem. Eng. J. 266 (2015) 213.